JAM-2 siRNA intracellular delivery and real-time imaging by proton-sponge coated quantum dots

Lifeng Qi,*[ab] Weijun Shao[a] and Donglu Shi[bc]

In this study, proton-sponge coated quantum dots were prepared by using amphipol PMAL, grafted with polyethylenimine (PEI) as an encapsulation polymer. The QD-PMAL-PEI nanoparticles showed low cytotoxicity and superior gene silencing efficiency in serum-containing medium against junctional adhesion molecule-2 (JAM-2), which is over-expressed in glioma cells. Confocal microscopic analysis showed efficient siRNA intracellular release. In particular, QD-mediated JAM-2 knockdown was reported for the first time to facilitate inhibition of glioma cell migration. Furthermore, the Notch pathway served as the target for the JAM-2 gene function, confirmed by downregulation of its downstream genes HES1 and HES5. The unique proton-sponge coated QDs can serve as multifunctional siRNA carriers for efficient gene silencing and real-time intracellular imaging, and provide a base for design of novel efficient siRNA delivery carriers with high biocompatibility.

1 Introduction

RNA interference (RNAi) is a key technology for sequence-specific suppression of genes. Its potential applications of synthetic siRNA have been considered for treatment of various diseases, including cancer, in recent years.[1,2] However, therapeutic applications of siRNA are still limited due to poor cellular uptake and accelerated degradation in biological fluids.[3] Most current transfection reagents, including nanoparticle-based carriers, have been used with RNAi in a serum free medium for their protection of siRNA from nuclease degradation. Lack of efficient delivery system with stable siRNA *in vivo* and high specificity to the desired tissue site is still a challenge for RNAi therapy.[4] The current approaches in siRNA delivery include liposomes,[5,6] polymers,[7] peptides,[8] and virus-based vectors *etc.*[9] However, these carriers are not fluorescent, therefore unable to monitor the siRNA delivery process. Typical strategies to track siRNA delivery include monitoring fluorescently end-modified siRNA[10] or co-transfecting reporter plasmids.[11] But these methods experienced rapid photobleaching, incapable of simultaneous monitoring of multiple siRNA molecules and insensitive to different heterogeneous siRNA delivery. Recently, quantum dots have been used as co-transfection reagent[12] or delivery system for siRNA delivery tracking.[13] On the other hand, these QDs such as L-arginine[14] or peptides[15] modified QDs suffer from limited transfection efficiency. High transfection efficiency is particularly required for high siRNA concentration at 100 nM.[16]

In our previous work, we developed a proton sponge polymer[17] and amphipol PMAL[18] coated mono-dispersed QDs for siRNA delivery. In this study, we report the proton-sponge coated QDs for further improvement of silencing efficiencies. The proton-sponge coated QDs are prepared based on ligand-exchange reactions and the endosome-disrupting polymers as amphipol PMAL, grafted with hyperbranched polyethylenimine (PEI).

JAM-2 is a part of a subfamily of junctional adhesion molecules (JAMs) comprising JAM-A, JAM-2 (JAM-B), and JAM-3 (JAM-C).[19] JAM-2 is specifically enriched in cell–cell contacts at the level of the tight junction,[20] and highly expressed in lymphatic and vascular endothelial cells, mostly in high endothelial venules (HEVs).[21,22] JAM-2 is preferentially expressed in the endothelium of arterioles in and around tumors and sites of inflammation.[23] Recently, JAM-2 was found to be aberrantly expressed in glioma, the monoclonal antibodies blocking JAM-2/3 interaction were also found to impair *in vivo* glioma growth and invasion.[24]

In this study, JAM-2 was found to be over-expressed in glioma by IHC (immunohistochemistry) assay. The intracellular JAM-2 siRNA delivery was achieved in real-time imaging mediated by proton-sponge coated quantum dot. This delivery system has been found to be particularly suitable at 5 nM siRNA concentration in serum containing medium. The gene silencing efficiency against JAM-2 expression reached more than 90%. Moreover, JAM-2 knockdown was reported for the first time that improves glioma cell migration inhibition by the Notch pathway.

[a]*Zhejiang California Nanosystems Institute, Zhejiang University, No. 268, Kaixuan Road, Hangzhou, 310029, China*

[b]*The Institute for Biomedical Engineering and Nano Science, School of Medicine, Tongji University, 67 Chifeng Road, Shanghai, 200092, China. E-mail: leonqi168@163.com; Fax: +86-021-65983706; Tel: +86-021-65983706-815*

[c]*School of Electronic and Computing Systems, University of Cincinnati, Cincinnati, OH 45221, USA*

2 Experimental section

Materials

All unspecified chemicals were purchased from Sigma Aldrich (USA) and used without additional purification. Biopsies of glioma and normal brain tissue from patients were collected during surgery in Second Affiliated Hospital of Zhejiang University. Glioma cells U251, A172, and U87MG were obtained from Shanghai cell bank. The cells were routinely grown at 37 °C in a 90% humidified atmosphere with 5% CO_2 (in air) in 25 cm^2 culture flasks (Corning Inc, USA) in Dulbecco's Modified Eagle's Media (DMEM, HyClone Inc, USA) with 10% of fetal bovine serum (HyClone Inc, USA) and 1% of penicillin streptomycin solution (HyClone Inc, USA). The anti-JAM-2 monoclonal antibody and GAPDH monoclonal antibody were obtained from Abnova (Taiwan, China). JAM-2 siRNA including siRNA labeled with AlexaFluor488 (AF488) and non-targeting siRNA were purchased from Dharmacon (USA). A tabletop ultracentrifuge (Beckman TL120) was used for nanoparticle purification and isolation. Confocal fluorescence images were obtained with a confocal microscope (Zeiss LSM 510, Germany) equipped with DPSS, argon, and He/Ne lasers with lines at 405, 458, 488, 543, and 633 nm. Multicolor gel images were acquired with a macro-imaging system (Lightools Research, Encinitas, CA). A Tecan Safire2 plate reader (Switzerland) was used for the cytotoxicity measurements based on MTT assays.

Immunohistochemistry (IHC)

SABC method was used to detect the expression of JAM-2 protein in glioma tissue. The IHC was strictly followed according to the manufacturer's instructions (Boster, Wuhan, China). Briefly, the tissue slices were incubated in 3% H_2O_2 and blocked with 5% BSA. They were then incubated with anti-JAM-2 antibody (1 : 200), biotin-conjugated second antibody (1 : 1000), and SABC sequentially.

Synthesis of QDs

The TOPO-capped CdSe and PMAL-capped QDs were prepared using a method reported in our previous work.[18] QD-PMAL-PEI were made by surface modification of the PMAL-QDs with branched PEI (25 kDa, Sigma) in PBS by using a modified EDC–NHS reaction, at starting molar ratio of PMAL-QDs to PEI as 1 : 100. The prepared QD-PMAL-PEI nanoparticles were purified twice by ultracentrifuge at 45 000 rpm for 30 min. The synthesized QDs were dissolved in PBS for further experiments.

Characterization

The dynamic radii and zeta potential of the QDs were measured by using a nanoparticle size analyzer (Malvern 2000, Malvern, England). The electrophoretic mobility of the prepared nanoparticles was determined by 0.8% agarose gel in TBE buffer at 100 mV for 30 min. The morphology and core sizes of QDs and QD–siRNA were studied by TEM (JEOL. Ltd Inc, Japan). The QDs and QD–siRNA solutions were dropped onto a copper net and observed by TEM after dehydration. A UV-2450 spectrophotometer (Shimadzu, Columbia, MD) and a Fluoromax4 fluorometer (Horiba Jobin Yvon, Edison, NJ) were used to characterize the absorption and emission spectra of the QDs.

siRNA loading efficiency

siRNA targeting JAM-2 (10 pmol) was incubated for 20 min with QDs of 5, 2.5, 1.25, 0.625, 0.313, 0.156 and 0.078 pmol to achieve QD–siRNA molar ratios of 1 : 2, 1 : 4, 1 : 8, 1 : 16, 1 : 32, 1 : 64, and 1 : 128, respectively. Agarose gel electrophoresis at 0.8% in TBE buffer was used to separate and quantify the unbound siRNA.

Cytotoxicity assay

Standard MTT assay was performed to determine the cytotoxicity of the QD-PMAL-PEI and QD–siRNA complexes. Briefly, cells were plated at a density of 2×10^4 cells per well in 96-well flat-bottomed microtiter plates (100 µL of cell suspension per well). 5 nM QDs and 10 nM siRNA were used to form transfection complexes. The cells were incubated with different amount of QDs and QD–siRNA complexes at 37 °C for 24 h, 48 h, and 72 h respectively. They were washed with PBS three times. 50 µL MTT was added in each well. After another four hours' incubation, the cells were washed and 100 µL DMSO were added to each well to dissolve unsolved MTT. The absorbance of the converted dye was measured at the wavelength of 570 nm. The experiments were repeated at least three times. The cell viability was calculated using the following formula: the average A value of experimental group/average $= A$ value of control group $\times$ 100%.

Laser confocal microscopy image analysis

The U251 cells were seeded in a laser confocal microscopy 35 mm^2 Petri dish (MatTek, USA) at a density of 1.0×10^5 cells and maintained for 48 h. Two different complexes, QD–siRNA^{AF488}, were prepared in serum-containing medium and incubated for 15 min at room temperature. The cells were transfected with the QD–siRNA complexes and incubated for different time intervals (0 min, 30 min and 6 h). After transfection, the medium was discarded and the cells were washed three times with $1 \times$ PBS. Confocal images were obtained at each time point using Leica TCS SP5 confocal laser scanning microscope (Leica Inc., USA). To acquire fluorescence signal, each sample was excited at 450 nm with an Ar laser. A fluorescence signal of AF488-siRNA was detected at 488 nm and the QD-PMAL-PEI signal was obtained at 605 nm.

Cells transfection procedures

Cellular transfection of siRNA was performed using QDs and commercial transfection reagents Lipofectamine™ RNAiMAX (Invitrogen, USA). For siRNA transfection, cells were trypsinized with 0.25% of trypsin solution (HyClone Inc, USA) for 3 min at 37 °C. 1×10^4 cells per well were subsequently plated into 24-well plates (Corning Inc, USA) overnight to achieve 60–80% confluence. The cultured cells were washed with $1 \times$ PBS and incubated for 30 min with complete medium serum-containing DMEM and 10% FBS. Lipofectamine™ RNAiMAX (1 µL per well)

were diluted in 50 μL of DMEM and were incubated for 15 min at room temperature. For QD-PMAL-PEI transfection, different amounts of QDs were first added in complete medium-containing serum instead of serum free medium. 50 μL of DMEM with different amounts of siRNA against JAM-2 (Dharmacon Inc, USA) was mixed with QDs to form transfection agents, and incubated for another 20 min at room temperature. Immediately before transfection, 500 μL of complete medium was added to QD–siRNA complexes and mixed by pipetting. The QD–siRNA complexes diluted in medium were added to each well, and the cells were incubated at 37 °C for 48 h in a CO_2 incubator. RNA or protein was extracted from the transfected cells for RT-PCR or Western blotting.

Real-time fluorescence quantitative PCR (RTFQ-PCR)

JAM-2 siRNA-treated cells were washed with PBS and lysed in 1.0 mL of RNAiso Plus (TaKaRa Inc, Japan) and total RNA was isolated. 1 mg RNA was used in reverse transcription with a PrimeScript RT reagent kit (TaKaRa Inc, Japan). cDNA was premixed by procedures of SYBR premix Ex TaqTM (TaKaRa Inc, Japan). For JAM-2 mRNA amplification, the forward and reverse primers were 5′ TCTTTTGGGGCAGAAAACC-3′ and 5′-AAGATGGCGAGGAGGAGC-3′. For GAPDH, the forward and reverse primers were 5′-AAATCGTGCGTGACATTAA-3′ and 5′-CTCGTCATACTCCTGCTTG-3′. RTFQ-PCR was performed directly in PCR tubes through a Real-Time PCR Detection System (CFX96, Biorad) with the following parameters: 30 s at 95 °C, 40 cycles consisting of 10 s at 95 °C, 30 s at 60 °C, and 10 s at 72 °C The CT values of melt cures were measured automatically.

Western blotting

Cells were lysed using RIPA protein extraction reagent (Pierce Inc, USA). The lysates were separated by centrifugation at 12 krpm, 4 °C for 10 min on an Eppendorf 5417R centrifuge (Eppendorf Inc, Germany). Supernatants were then collected, and the protein concentration was measured by a standard BCA protein assay kit (Thermo Pierce, USA). Equal amounts of protein were loaded and separated on 12% sodium dodecyl sulfate poly-acrylamide gel electrophoresis (SDS-PAGE) and were transferred for 1 h at 150 V using Bio-Rad Mini-PROTEAN4 (Bio-Rad Inc, USA) to nitrocellulose membranes (Bio-Rad Inc, USA) in transfer buffer (25 mM Trise HCl, 200 mM glycine, 10% methanol) and blocked with 5% milk blocking buffer for 2 h on a horizontal shaker. The blocked membranes were incubated with 1 : 2000 JAM-2 mouse monoclonal antibodies (Abnova, Taiwan, China), diluted in 5% milk blocking buffer. The membranes were washed in Tween–Tris Buffered Saline [TTBS: 0.1% Tween-20 in 100 mM Tris HCI (pH 7.5), 0.9% NaCl] and probed with horseradish peroxidase (HRP) labeled goat anti-mouse secondary antibodies (Santa Cruz Inc, USA), diluted at 1 : 5000 in 5% milk blocking buffer. The blots were developed by using an ECL kit (Amersham Inc, USA). The membranes were exposed to Kodak X-OMAT film for 10–30 s for data acquisition and developed using a conventional film developing machine.

Effects of JAM-2 silence on glioma cell migration

Cell migration assay was performed using Transwell chambers (6.5 mm diameter; 8 μm pore size polycarbonate membrane) obtained from Corning. 2×10^5 U251 cells 24 h after transfection with QD-JAM-2 siRNA in 0.2 mL FBS-free DMEM were loaded in the upper chamber, whereas the lower chamber was placed with 0.5 mL medium containing 15% FBS. After 48 h incubation, the total number of cells that migrated into the lower chamber was counted under a light microscope at ×400.

Statistical analysis

Statistical analysis of data was performed with the one-factor analysis of variance (SPSS software, version 13.0, SPSS Inc). The results were expressed as mean ± SD (standard deviation), and $P < 0.05$ was considered to be statistically significant. All statistical tests were two-sided.

3   Results and discussion

Rational design of siRNA delivery carriers plays an important role in successful RNAi. The key requirements for siRNA carriers must be met to avoid degradation in the extracellular milieu. These carriers must be targeted on cell surfaces for intracellular uptake, unpacking from carriers, and ultimately entering RISC where unwinding and pairing of the antisense strand with native mRNA take place. Therefore, surface coating of nano carriers is essential in siRNA delivery.[25]

In order to develop efficient siRNA and highly stable delivery system ideally suited for *in vivo* studies, QD-PMAL-PEI was prepared for its advantages of amphipol[18] and cell-penetrating features of PEI. Amphipol PMAL was used to solubilize hydrophobic QDs. PEI molecules were conjugated with PMAL coated QDs in order to enhance the endosomolytic effects of QDs through the so-called "proton sponge effect." PMAL encapsulated QDs were prepared using a method previously reported.[18] QD-PMAL-PEI is synthesized by conjugating branched PEI (25 kDa) with PMAL-QDs. As shown in Scheme 1, amphipol PMAL is used to solubilize hydrophobic QDs initially. PEI is then conjugated with PMAL coated QDs to obtain QD-PMAL-PEI. siRNA molecules subsequently bind onto QD-PMAL-PEI surface by electrostatic interaction to form transfection complexes.

3.1   Characterization of QD-PMAL-PEI

The particle size, surface charge, the adsorption and emission spectra of Original QDs, QD-PMAL and QD-PMAL-PEI were
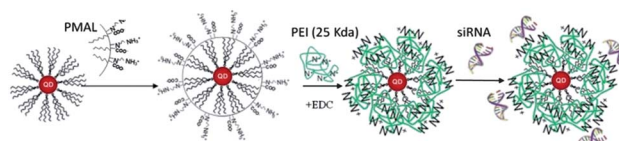
Scheme 1 Schematic representation of QD-PMAL-PEI synthesis for siRNA delivery.
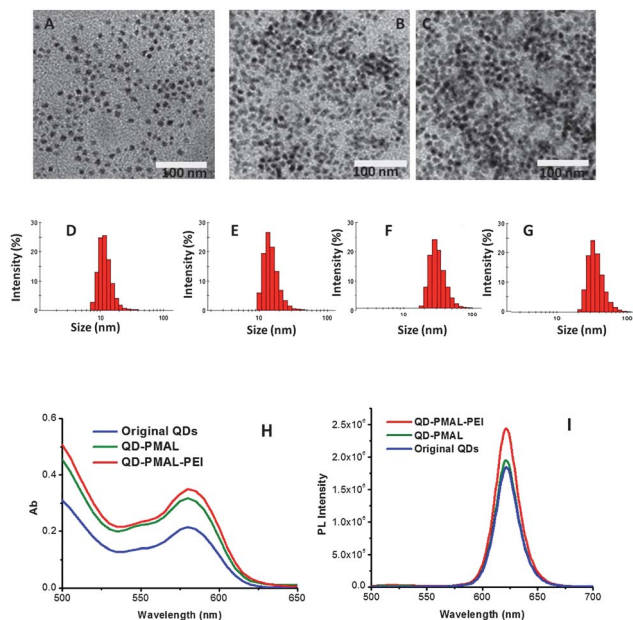
Fig. 1 Characterization of original QDs, QD-PMAL and QD-PMAL-PEI. TEM photographs of Original QDs (A), QD-PMAL (B) and QD-PMAL-PEI (C); hydrodynamic diameters of original QDs (D), QD-PMAL (E), QD-PMAL-PEI in PBS (F) and in serum containing medium (G); absorption spectra (H) and emission spectra (I) of original QDs, QD-PMAL and QD-PMAL-PEI.

Fig. 2 Electrophoresis analysis and zeta potential of QD-PMAL-PEI and QD–siRNA complexes.

characterized respectively. TEM photographs (Fig. 1A–C) show that original QDs exhibit mono-dispersion with core size about 10 nm, no significant size increase on QD-PMAL and QD-PMAL-PEI. The dynamic laser scattering (DLS) analysis is shown in Fig. 1D–G. As can be seen in this figure, the hydrodynamic diameters of original QDs, QD-PMAL and QD-PMAL-PEI are 12.1 ± 0.5, 14.7 ± 0.8 nm and 32.5 ± 3.5 nm, respectively. The UV absorption spectra (Fig. 1H) of three kinds of QDs showed no significant change on absorption profile, while the emission spectra (Fig. 1I) of them showed enhanced fluorescent intensity of QD-PMAL-PEI at the same concentration of QDs. This indicated the PEI modification on PMAL polymer coated QDs can improve their photo-stability.

In order to study the stability of QD-PMAL-PEI in serum, the hydrodynamic diameter and zeta potential of QD-PMAL-PEI dispersed in serum containing medium were determined. The particle size of QD-PMAL-PEI increases to 37.2 ± 4.1 nm (Fig. 1G), while the zeta potential of QD-PMAL-PEI decreases from 34.7 ± 3.6 mV in PBS to 26.2 ± 4.5 mV in serum-containing medium (Fig. 2). Higher surface charge of QD-PMAL-PEI is confirmed by electrophoresis (Fig. 2) of the two positively charged QDs together with negatively charged QDs encapsulated by DSPE-PEG (1,2-distearoyl-*sn*-glycero-3-phosphoethanolamine-*N*-[carboxy(polyethylene glycol)-2000], Avanti Polar Lipids INC., US) polymer. Quantum dots have been reported to interact with bovine serum protein to form QD–BSA complexes.[26] The increase of particle size and decrease of zeta potential of QD-PMAL-PEI in serum containing medium is attributed to the interaction between positively charged QDs and negatively charged BSA in serum.
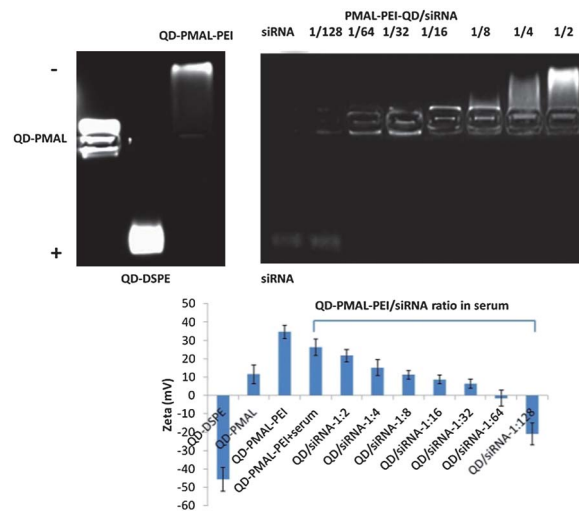
3.2 siRNA binding capacity of QD-PMAL-PEI

siRNA binding efficiency of QDs was determined by agarose gel electrophoresis. Results show that the synthesized proton-sponge coated QDs can bind siRNA molecules with high efficiency, at molar ratio of QDs to siRNA more than 1 : 32 (Fig. 2). The zeta potential of QD–siRNA decreases gradually with the increase of molar ratio of QDs to siRNA. Efficient siRNA delivery requires the positive charge of QD–siRNA complexes, but excessive positive charge can prevent the release of siRNA from complexes. The optimized molar ratio of QDs to siRNA is in the range from 1 : 1 to 1 : 4.

3.3 Cytotoxicity of QDs and QD–siRNA complexes

The cytotoxicities of QD-PMAL-PEI and QD–siRNA complexes were measured by standard MTT assay in U251 cells. The cells were treated with different amounts of QDs ranging from 0 to 16 nM in serum free and serum-containing medium for 24 h. For the cytotoxicity of QD–siRNA complexes, 5 nM QDs and 10 nM siRNA were applied. Cells were treated with QD–siRNA complexes for 48 h and 72 h, the cell viability was then determined respectively. As shown in Fig. 3, QD-PMAL-PEI has significantly low cytotoxicity in serum-containing medium compared with serum free medium. The cell viability of 8 nM QDs in serum-containing medium is higher than 87%, while that is 61% in serum free medium. As the QDs concentration reaches 16 nM, the cell viability is found to be higher than 60% in serum-containing medium. The work concentration of QDs for efficient JAM-2 siRNA transfection is only 5 nM. The QD–siRNA complexes do not show pronounced cytotoxicity in serum-containing medium (Fig. 3).

Low cytotoxicity of nano carriers is highly preferred for efficient RNAi. Although PEI polymer as a gene carrier is well known for its high cytotoxicity, here QD-PMAL-PEI and complexes with siRNA showed negligible cytotoxicity. Their low cytotoxicity is attributed to the zwitterionic surface charge from
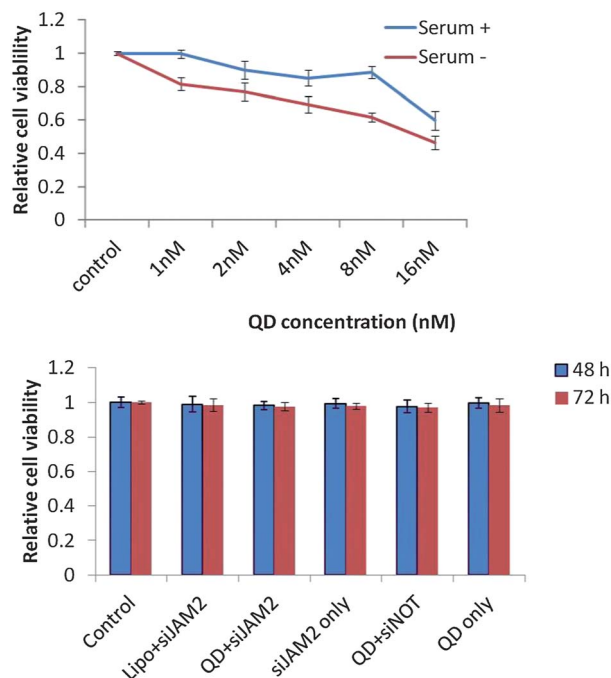
Fig. 3 Cytotoxicity of QD-PMAL-PEI and QD–siRNA complexes.

amphipol coating, low concentration use of final complexes as 5 nm, and neutralized surface charge due to siRNA adsorption onto the nanoparticles. Recent report on siRNA delivery by PEI modified gold-chitosan nanosystem also showed low cytotoxicity due to sufficient siRNA loading.[27]

3.4 Intracellular imaging of QD–siRNA complexes

Confocal microscopy was used to monitor the time-dependent accumulation of QD–siRNA^{AF488} complexes in U251 cells. The concentration of both QDs and siRNA is 5 nM. The QD–siRNA^{AF488} complexes were attached to the cell membrane immediately after added in cell medium, and a bright red ring standing for QDs fluorescence was observed. After internalization, green fluorescence from siRNA^{AF488} increases significantly at a time dependent mode (Fig. 4), indicating that the siRNA
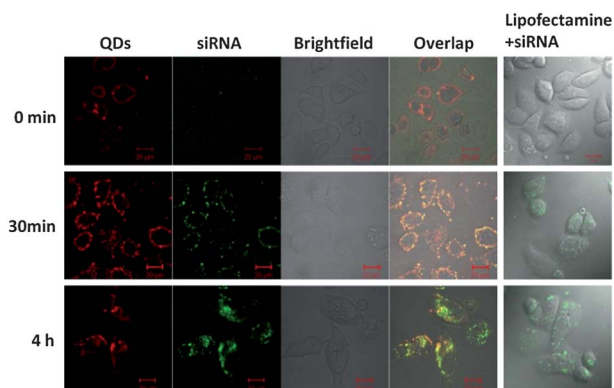
molecules begin to dissociate from QD–siRNA^{AF488} complexes step by step. Until 6 h, most siRNA molecules have already diffused inside cytoplasm. Lipofectamine mediated siRNA^{AF488} delivery was used as positive control, and observed in different time intervals comparable with that of the QDs group. Lipofectamine–siRNA complexes showed much lower intracellular siRNA release even after 4 hours' incubation. This indicates that lipofectamine required much longer time for interaction with cell membrane to achieve sufficient intracellular siRNA delivery, thus leading to lower gene silencing efficiency.

Sufficient siRNA unpacking from carriers is an important step during RNAi. Particle size has been reported to have effects on receptor-mediated endocytosis and 40–60 nm was suggested to be the optimal size range for enhanced uptake.[28] As described earlier, the hydrodynamic particle size of QD-PMAL-PEI increases to about 40 nm when dispersed in serum containing medium, which was responsible for higher intracellular uptake of QDs.

3.5 Gene silencing efficiency of QD–siRNA complexes

Different amounts of QDs and siRNA against JAM-2 (siJAM-2) were used to study the knockdown efficiency. 5 nM QDs and 10 nM siJAM-2 in serum-containing medium were investigated for silencing efficiency by Western blot. Lipofectamine was used as a positive control. All transfection was performed in complete medium with serum.

The gene silencing efficiency of QDs was investigated by RT-PCR and Western blot experiments. Lipofectamine was used as positive control. Different amount of JAM-2 siRNA was mixed with various concentrations of QDs to form transfection agents in serum-containing medium. Compared with the non-targeting siRNA control, the expression level of JAM-2 mRNA was reduced to $42 \pm 6\%$, $13.5 \pm 3\%$, and $14 \pm 7.5\%$ respectively, when siRNA concentration was 5 nM, 10 nM, and 15 nM respectively, and the QDs concentration was kept at 5 nM. For the siRNA concentration at 15 nM, the amount of QDs amount can be reduced to as low as 3 nM to reach $65 \pm 9.7\%$ knockdown efficiency. When 7.5 nM QDs and 15 nM siRNA were applied, silencing efficiency increased to $91 \pm 5.3\%$. For siRNA
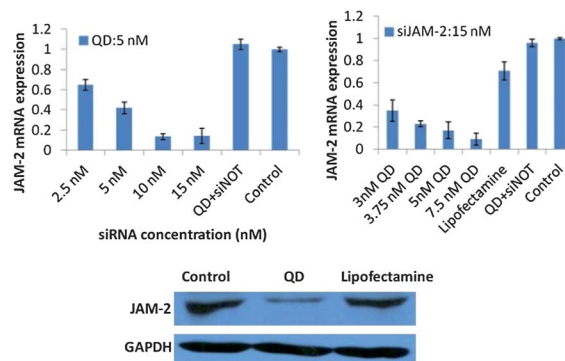

Fig. 4 Real-time imaging of siRNA^{AF488} release from QD-PMAL-PEI by confocal microscopy.

Fig. 5 Gene silencing efficiency of PMAL-PEI-QD against JAM-2 at mRNA and protein expression level.

658 | J. Mater. Chem. B, 2013, **1**, 654–660

This journal is © The Royal Society of Chemistry 2013

concentration at 15 nM, the JAM-2 mRNA of lipofectamine–siRNA transfected cells remain $30 \pm 5\%$ in serum containing medium (Fig. 5). Western blot shows higher silencing efficiency for 5 nM QDs and 10 nM siRNA in serum containing medium, compared with lipofectamine group with the same concentration of siRNA.

Based on the above results, a novel delivery system is developed with the required minimum siRNA concentration at 5 nM, especially suited for transfection in serum-containing medium. The efficient intracellular siRNA release from the proton-sponge coated quantum dots contribute to high silencing efficiency.

3.6 Over-expression of JAM-2 in glioma

The expression of JAM-2 in a series of human glioma cell lines including U251, U87MG, and A172 cells was analyzed by Western blot. It was found that the three cell lines tested are all JAM-2 positive (Fig. 6A). It was also found that JAM-2 is over-expressed in glioma tumors (Fig. 6B) compared to non-tumoral human brain tissue (Fig. 6C) obtained by surgery from patients as detected by IHC.

3.7 Cell migration assay and potential mechanism

Cell migration was studied by use of Transwells chambers. As shown in Fig. 7, after JAM-2 siRNA delivery by QD-PMAL-PEI, glioma cell migration is inhibited significantly compared with control cells without any treatment. A reduction of 80% in glioma cell migration is observed in cells after transfected with QD–siRNA complexes. Glioblastoma (GBM) is a kind of highly invasive brain tumor, the aggressive features show limited response to conventional therapies. Inhibition of glioma cell migration provides the possibility to overcome the glioma metastasis.

In order to investigate the signal pathway involved in inhibition of cell migration by JAM-2 knockdown, the effects of JAM-2 gene silencing on the Notch pathway were studied. The Notch pathway was found to be inhibited due to JAM-2 knockdown by siRNA delivery. This has been verified by the deregulated gene expression of Notch1 receptor and their downstream targets HES1 and HES5.[29] VEGF expression is also inhibited significantly after JAM-2 downregulation (Fig. 7). Notch signaling

Fig. 6 Expression of JAM-2 in different glioma cell lines (from left to right side: U251, U87MG, and A172), and expression in clinical glioma tissue (A) and non-tumoral tissue (B).
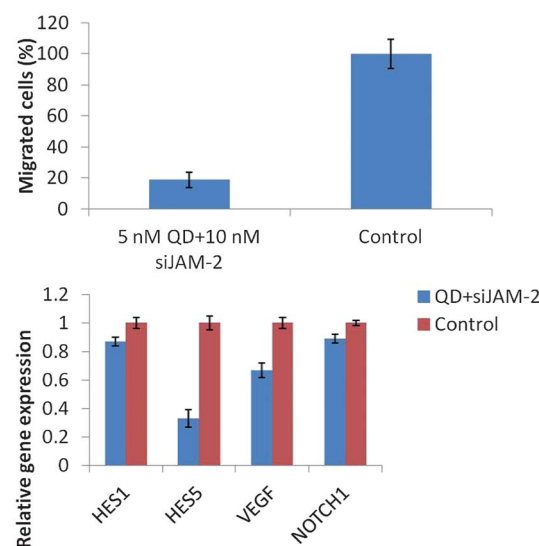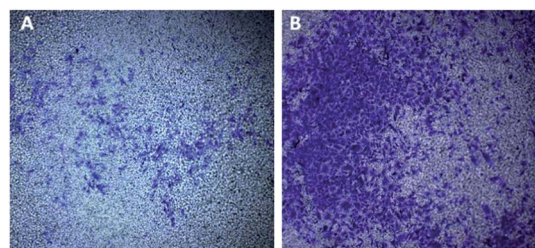

Fig. 7 Effects of JAM-2 silencing mediated by QD-PMAL-PEI on glioma cell migration ((A): JAM-2 knockdown by QD-PMAL-PEI; (B): control) and gene expression of Notch1 pathway downstream genes and VEGF.

plays an important role in glioma migration and invasion.[30] VEGF receptor is an important biomarker over-expressed in glioma, VEGF inhibitors have been applied in clinical therapies, and blockage of Notch signaling could improve the efficacy of VEGF inhibitors.[31] Knockdown of JAM-2 leads to inhibition of the Notch signal pathway, thus inhibiting glioma migration. These findings provide the first evidence that JAM-2 is a promising target for the development of new anti-metastasis reagent for cancer gene therapy.

4 Conclusions

A novel class of proton-sponge coated QDs, PMAL grafted with PEI loaded with CdSe/ZnSe QDs have been prepared through direct ligand-exchange reactions and surface modifications as multifunctional complexes for siRNA delivery and real-time intracellular imaging. Systematic biological experiments show that QD-PMAL-PEI exhibit low cytotoxicity. These QD–siRNA complexes can be readily internalized into cells confirmed by flow cytometric and confocal microscopic analyses. Importantly, superior gene silencing efficiency (more than 90%) is achieved using the QD–siRNA complexes as determined by real-time fluorescence quantitative PCR. In addition, the QD–siRNA complexes, which target JAM-2 oncogene, can inhibit U251 cells migration significantly. It is worth noting that all transfection experiments of QD-PMAL-PEI were conducted in serum-containing medium. The QDs show superior gene silencing
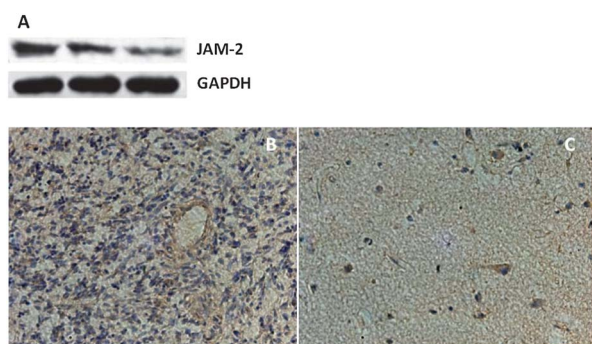
properties compared with lipofectamine. The minimum concentration of siRNA for transfection is only 5 nM, much lower than that of others transfection reagents previously reported.[5–8] The dual modality of QD–siRNA complexes allows real-time tracking of QDs and siRNA release during siRNA delivery. The unique properties of proton-sponge coated QDs can be further optimized *in vivo* for tumor targeting, drug delivery and simultaneous imaging due to their high stability and superior silencing efficiency in serum-containing environments.

Acknowledgements

Notes and references

1 P. M. Waterhouse, M. B. Wang and T. Lough, *Nature*, 2001, **411**, 834.

2 A. K. Ameln, A. Muschter, S. Mamlouk, J. Kalucka, I. Prade, K. Franke, M. Rezaei, D. M. Poitz, G. Breier and B. Wielockx, *Cancer Res.*, 2011, **71**, 3306.

3 J. B. Lee, J. Hong, D. K. Bonner, Z. Poon and P. T. Hammond, *Nat. Mater.*, 2012, **11**, 316.

4 M. S. Shim and Y. J. Kwon, *FEBS J.*, 2010, **277**, 4814.

5 M. Jayaraman, S. M. Ansell, B. L. Mui, Y. K. Tam, J. Chen, X. Du, D. Butler, L. Eltepu, S. Matsuda, J. K. Narayanannair, K. G. Rajeev, I. M. Hafez, A. Akinc, M. A. Maier, M. A. Tracy, P. R. Cullis, T. D. Madden, M. Manoharan and M. J. Hope, *Angew. Chem., Int. Ed.*, 2012, **51**, 8529.

6 D. N. Nguyen, K. P. Mahon, G. Chikh, P. Kim, H. Chung, A. P. Vicari, K. T. Love, M. Goldberg, S. Chen, A. M. Krieg, J. Chen, R. Langer and D. G. Anderson, *Proc. Natl. Acad. Sci. U. S. A.*, 2012, **109**, E797.

7 J. Hoyer and I. Neundorf, *Acc. Chem. Res.*, 2012, **45**, 1048.

8 C. Ornelas-Megiatto, P. R. Wich and J. M. Fréchet, *J. Am. Chem. Soc.*, 2012, **134**, 1902.

9 C. E. Ashley, E. C. Carnes, G. K. Phillips, P. N. Durfee, M. D. Buley, C. A. Lino, D. P. Padilla, B. Phillips, M. B. Carter, C. L. Willman, C. J. Brinker, C. Caldeira Jdo, B. Chackerian, W. Wharton and D. S. Peabody, *ACS Nano*, 2011, **5**, 5729.

10 R. H. Mo, J. L. Zaro and W. C. Shen, *Mol. Pharmaceutics*, 2012, **9**, 299.

11 H. Chang Kang and Y. H. Bae, *Biomaterials*, 2011, **32**, 4914.

12 W. B. Tan, S. Jiang and Y. Zhang, *Biomaterials*, 2007, **28**, 1565.

13 J. M. Li, Y. Y. Wang, M. X. Zhao, C. P. Tan, Y. Q. Li, X. Y. Le, L. N. Ji and Z. W. Mao, *Biomaterials*, 2012, **33**, 2780.

14 J. M. Li, M. X. Zhao, H. Su, Y. Y. Wang, C. P. Tan, L. N. Ji and Z. W. Mao, *Biomaterials*, 2011, **32**, 7978.

15 C. Kim, Y. Lee, J. S. Kim, J. H. Jeong and T. G. Park, *Langmuir*, 2010, **26**, 14965.

16 J. Jung, A. Solanki, K. A. Memoli, K. Kamei, H. Kim, M. A. Drahl, L. J. Williams, H. R. Tseng and K. Lee, *Angew. Chem., Int. Ed.*, 2010, **49**, 103.

17 M. V. Yezhelyev, L. Qi, R. M. O'Regan, S. Nie and X. Gao, *J. Am. Chem. Soc.*, 2008, **130**, 9006.

18 L. Qi and X. Gao, *ACS Nano*, 2008, **2**, 1403.

19 G. Bazzoni, *Curr. Opin. Cell Biol.*, 2003, **15**, 525.

20 I. Martin-Padura, S. Lostaglio, M. Schneemann, L. Williams, M. Romano, P. Fruscella, C. Panzeri, A. Stoppacciaro, L. Ruco, A. Villa, D. Simmons and E. Dejana, *J. Cell Biol.*, 1998, **142**, 117.

21 M. Aurrand-Lions, C. Johnson-Leger, C. Wong, L. Du Pasquier and B. A. Imhof, *Blood*, 2001, **98**, 3699.

22 D. Palmeri, A. Van Zante, C.-C. Huang, S. Hemmerich and S. D. Rosen, *J. Biol. Chem.*, 2000, **275**, 19139.

23 T. W. Liang, H. H. Chiu, A. Gurney, A. Sidle, D. B. Tumas, P. Schow, J. Foster, T. Klassen, K. Dennis, R. A. DeMarco, T. Pham, G. Frantz and S. Fong, *J. Immunol.*, 2002, **168**, 1618.

24 M. Tenan, M. Aurrand-Lions, V. Widmer, A. Alimenti, K. Burkhardt, F. Lazeyras, M. C. Belkouch, P. Hammel, P. R. Walker, M. A. Duchosal, B. A. Imhof and P. Y. Dietrich, *Glia*, 2010, **58**, 524.

25 N. Singh, A. Agrawal, A. K. Leung, P. A. Sharp and S. N. Bhatia, *J. Am. Chem. Soc.*, 2010, **132**, 8241.

26 D. Wu, Z. Chen and X. Liu, *Spectrochim. Acta, Part A*, 2011, **84**, 178.

27 L. Han, J. Zhao, X. Zhang, W. Cao, X. Hu, G. Zou, X. Duan and X. Liang, *ACS Nano*, 2012, **6**, 7340.

28 W. Jiang, Y. S. KimBetty, J. T. Rutka and W. C. Chan, *Nat. Nanotechnol.*, 2008, **3**, 145.

29 X. P. Zhang, G. Zheng, L. Zou, H. L. Liu, L. H. Hou, P. Zhou, D. D. Yin, Q. J. Zheng, L. Liang, S. Z. Zhang, L. Feng, L. B. Yao, A. G. Yang, H. Han and J. Y. Chen, *Mol. Cell. Biochem.*, 2008, **307**, 101.

30 X. Zhang, T. Chen, J. Zhang, Q. Mao, S. Li, W. Xiong, Y. Qiu, Q. Xie and J. Ge, *Cancer Sci.*, 2012, **103**, 181.

31 J. L. Li, R. C. Sainson, C. E. Oon, H. Turley, R. Leek, H. Sheldon, E. Bridges, W. Shi, C. Snell, E. T. Bowden, H. Wu, P. S. Chowdhury, A. J. Russell, C. P. Montgomery, R. Poulsom and A. L. Harris, *Cancer Res.*, 2011, **71**, 6073.